Resonant orbits for a spinning particle in Kerr spacetime

Sajal Mukherjee[1,*] and Santanu Tripathy[1,2,†]

[1]*Department of Physical Sciences, IISER-Kolkata, Mohanpur-741246, India*
[2]*Center of Excellence in Space Sciences India, IISER-Kolkata, Mohanpur-741246, India*

In the present article, we study the orbital resonance that corresponds to an extended object approximated up to the dipole order term in Kerr spacetime. We start with the Mathisson-Papapetrou equations under the linear spin approximation and primarily concentrate on two particular events: first, when the orbits are nearly circular and executing a small oscillation about the equatorial plane and second, a generic trajectory confined on the equatorial plane. While in the first case, all three fundamental frequencies, namely, radial Ω_r, angular Ω_θ, and azimuthal Ω_ϕ can be commensurate with each other and give rise to the resonance phenomenon, the later is only accompanied with the resonance between Ω_r and Ω_ϕ as we set $\theta = \pi/2$. We provide a detailed derivation in locating the prograde resonant orbits in either of these cases and also study the role played by the spin of the black hole. The implications related to spin-spin interactions between the object and black hole are also demonstrated.

I. INTRODUCTION

In the strong field regime where the effects of gravity are inescapable, the motion of test particles can be attributed to many nontrivial consequences such as precession, spiraling of orbits, resonance, chaos, and so on [1–6]. Even if these investigations related to the trajectories of test particles are not present-day concerns but rather contained with extensive literature spanned over last several years [7,8], there are relevant studies with possible observational aspects yet to be explored [9,10]. Regarding the observational implications, there are proposed mission such as The Laser Interferometer Space Antenna (LISA) which aims to probe extreme mass ratio binaries in the near future as well [11–13]. However, any attempt to explain the phenomenon that involves incomparable masses would require one to grasp the theoretical structure of particle trajectories as well. While in many cases, it is appropriate to consider that the lighter companion as a point test particle that moves along a geodesic trajectory, the addition of higher order moments may introduce larger accuracy in estimating any measurable quantities. These higher order moments can originate from the nontrivial internal structure of the body represented by its energy-momentum tensor $T^{\mu\nu}$ while their dynamics can be derived from the conservation equation $\nabla_\mu T^{\mu\nu} = 0$. By expanding $T^{\mu\nu}$ about a reference point located inside the object, say $z_\mu(t)$, the zeroth order term of

the conservation equation would produce the geodesic equation while the first order introduces the Mathisson-Papapetrou equations accordingly [14,15]. The next order contribution arise from the quadrupole moment and would be given by the Mathisson-Papapetrou-Dixon equations [16–18]. However, in the present article, we only consider the first order correction to the geodesic equations as introduced by the nonzero spin or dipole moment of the particle $S^{\mu\nu}$ given as [15]

$$S^{\mu\nu} = \int r^\mu \mathbf{T}^{0\nu} d^3x - \int r^\nu \mathbf{T}^{0\mu} d^3x, \tag{1}$$

with both μ and ν running from 0 to 3. The scaled energy-momentum tensor $\mathbf{T}^{0\mu} = \sqrt{-g}T^{0\mu}$, with g being the determinant of the metric, is integrated over the spacelike hypersurface represented by $t = $ constant slices. The dipole moment is computed about a reference point $z_\mu(t)$ while the distance between $z_\mu(t)$ and any given mass point is given by r^μ which contains no time component according to the definition.

From a theoretical standpoint, the astrophysical objects are likely to have a finite size and therefore it is appropriate to consider additional moments such as dipole, quadrupole, and so on. While particles with only mass monopole are named as monopole particles, the addition of dipole and quadrupole moment would introduce a pole-dipole, i.e., a spinning particle, and a pole-dipole-quadrupole particle, respectively. However, in the present context we shall only discuss some aspects of pole-dipole or spinning particles and not consider the quadrupole moment. The motion of a spinning particle constitutes an interesting problem and has

---

*Present address: The Inter-University Centre for Astronomy and Astrophysics, Post Bag 4, Pune-411007, India.
sajal@iucaa.in
†st12rs048@iiserkol.ac.in

been studied extensively in literature [19–22]. With the pioneering work by Papapetrou in 1951 [15], the early contributions from Mathisson [14], Ehlers and Rudolph [23] and Dixon [24] are also worth mentioning. In recent times, there have also been significant studies regarding several aspects of spinning particles and their nontrivial features [25–37]. For an excellent overview on the subject, we refer our readers to Refs. [38–40]. In one way, it emerges as an engaging theoretical implication with possible usefulness in explaining the motion of objects with nontrivial internal structure and also paves the way for an extreme mass ratio inspiral in general [41].

In the present article, we aim to study the resonant orbits for a spinning particle in the Kerr background, and for computational convenience, we restrict our discussions to two major aspects: first, the resonance between different small oscillation frequencies corresponding to nearly circular orbits close to the equatorial plane and second, the resonance between radial and azimuthal frequencies considering the trajectories are completely confined on the equatorial plane of the black hole. In the former, it is possible to encounter the resonance in between radial Ω_r and angular Ω_θ as well as azimuthal Ω_ϕ frequencies, while in the later, it is only between Ω_r and Ω_ϕ. Out of these three frequencies, the radial and angular are known as libration frequencies, while the later Ω_ϕ can be thought of as a rotational frequency. The correspondence between these frequencies would lead to the occurrence of resonance phenomenon in astrophysical scenarios. In particular, whenever the ratio of any of these frequencies becomes a rational fraction, the orbits become resonant. For example, with the $r\phi$ resonance, the principle equation is given as $\Omega_r/\Omega_\phi = n/m$, where both n and m are a rational number with no common divisor.

With the above motivation, let us now introduce the physical notion of resonance in astrophysical scenarios and also highlight its importance in the present context as well. Apart from astrophysical settings, the events like resonance are usually encountered in vibrations of strings and coupled oscillations [42]. For example, in case of a forced vibrating oscillator, the resonance becomes dominant whenever the natural frequency of the system becomes nearly equal to the frequency of the forced oscillation. Similar to this, the weakly coupled oscillators can also undergo resonance phases whenever their individual frequencies are comparable to each other. On the other hand, any external perturbation may introduce nonintegrability in the Hamiltonian and the system may encounter chaos. However, for a sufficiently small perturbation, the system may remain nearly integrable and the notion of a separability constant (also known as a Carter constant in the black hole spacetime) may still approximately exist [43–45]. In the case of a spinning particle with Tulczyjew-Dixon supplementary condition, the Carter-like constant can be defined as far as the $\mathcal{O}(S^2)$ terms are neglected [30,46–48]. However, for other supplementary conditions, the spin of

the particle may introduce chaos in the system [49,50]. Nonetheless, as the present analysis only considers the Tulczyjew-Dixon condition, the system can be considered integrable within the linear spin approximation. This would allow us to obtain the resonant orbits similar to the case of geodesic trajectories as given in Ref. [5]. It is of significant interest to locate the resonant orbits as it is likely that these orbits will witness the breakdown of phase space tori for the first time if the system undergoes any chaos [51–54].

Earlier in literature, several implications related to resonance activities were addressed in various aspects [55–57]. As already mentioned, the orbital dynamics in a Kerr black hole depends on three fundamental frequencies relating three spatial components and therefore, there could exists different types of resonant orbits. The $r\theta$ resonant orbits are studied in Ref. [5] whereas the $\theta\phi$ and $r\phi$ resonances are addressed in Refs. [57,56] respectively. In Refs. [56,57], the black hole kicks are also studied for an extreme mass ratio inspiral considering the lighter companion follows a geodesic orbit. For an investigation related to the resonance in between the spin precession frequencies and orbital frequencies of a spinning particle, we refer our readers to Ref. [58] for a better understanding. However, as far as the analysis in the present article is concerned, we would only consider the resonance between orbital fundamental frequencies of a spinning particle and the effect of the spin precession frequency is excluded.

The rest of the paper is organized as follows. In Sec. II, the basic governing equations of a spinning particle are introduced along with various implications such as spin supplementary condition and conserved quantities. These equations are exactly solved on the equatorial plane of the Kerr black hole and the effective radial potential is also obtained for further calculations. Following this in Sec. III, we introduce the machinery to obtain the fundamental frequencies and orbital resonance for any trajectory in a black hole's spacetime. In particular, we studied two different events corresponding to a spinning object: first, the small oscillation frequencies for a particle orbiting in nearly circular orbits close to the equatorial orbits and second, a general motion confined on $\theta = \pi/2 = $ constant plane. Section IV is devoted to exploring the resonance phenomenon related to the first case while in Sec. V, the $r\phi$ resonances are elaborately studied. In the later, the approximation technique, namely the Sochnev method, is employed to evaluate the integrals on the equatorial plane of the black hole. We conclude the article with a brief remark in Sec. VI.

II. MOTION OF A SPINNING PARTICLE IN A GRAVITATIONAL FIELD

The motion of a spinning particle is described by the Mathisson-Papapetrou equations

$$\frac{DP^a}{d\tau} = -\frac{1}{2} R^a_{bcd} \mathcal{U}^b S^{cd}, \qquad \frac{DS^{ab}}{d\tau} = P^a \mathcal{U}^b - P^b \mathcal{U}^a, \quad (2)$$

where P^a and $\mathcal{U}^a$ correspond to the four momentum and four velocity of the particle respectively, S^{ab} is the spin tensor of the extended object relating to the dipole moment, and R^a_{bcd} has the usual meaning of Riemann curvature tensors corresponding to the background geometry. Furthermore, it should be emphasized that the above set contains a total of 10 equations while we have 14 (6 from the spin, 4 from the four velocity, and 4 from the four momentum) unknowns to solve, and therefore, additional conditions are required. These are called spin supplementary condition s and in the present context, we shall employ the Tulczyjew-Dixon condition $S^{ij} P_j = 0$ to solve Mathisson-Papapetrou equations around the Kerr black hole [59]. While a supplementary condition only gives three independent constraints, the fourth comes from the choice of the time parametrization [60]. In the present article, we have employed the parametrization introduced in Ref. [23] and later employed in Refs. [30,32]. This is given as $P^i \mathcal{U}_i = -\mu$, where μ is the conserved mass as given by $P^i P_i = -\mu^2$. Let us now introduce the notion of spin vector S^i for simplified computations; it is related with the spin tensor as follows [30,32]:

$$S^i = \frac{1}{\mu\sqrt{-g}} \epsilon^{ijkl} P_j S_{kl}, \qquad (3)$$

where g is the determinant of the background metric. For the particle confined on the equatorial plane, it is convenient to assume that the spin vector follows $S^i = (0, 0, S^\theta, 0)$ which indicates that the spin is either parallel or antiparallel to the black hole's rotational axis.

In addition, the symmetries associated with the background geometry will give rise to the conserved quantities such as energy and momentum. The compact expression for any conserved quantity $\mathcal{C}$ related to a killing vector field $\mathcal{K}^i$ can be written as

$$\mathcal{C} = \mathcal{K}^i P_i - \frac{1}{2} S^{ij} \mathcal{K}_{i;j}, \qquad (4)$$

where the contribution from the spin can be easily spotted [61,62]. It should also be noted that the total spin per mass of the particle, i.e., $S^2 = (S^i S_i)/\mu^2$ is conserved along the trajectory of the particle as it can be established from the Tulczyjew-Dixon supplementary condition. With all this machinery, one should be able to solve the Mathisson-Papapetrou equations and also establish a relation between the four velocity and four momentum of the particle. In the present context, we only state the final results corresponding to the components of four velocity of the particle while the full derivations can be found in Ref. [32]. On the equatorial plane, these equations are given as

$$(\Sigma_s \Lambda_s \mathcal{U}^1)^2 = R_s = P_s^2 - \Delta\left(\frac{\Sigma_s^2}{r^2} + \{J_z - (a + S)E\}^2\right),$$

$$(\Sigma_s \Lambda_s \mathcal{U}^0) = a\left(1 + \frac{3S^2}{r\Sigma_s}\right)\{J_z - (a + S)E\} + \frac{r^2 + a^2}{\Delta} P_s,$$

$$(\Sigma_s \Lambda_s \mathcal{U}^3) = \left(1 + \frac{3S^2}{r\Sigma_s}\right)\{J_z - (a + S)E\} + \frac{a}{\Delta} P_s, \qquad (5)$$

where a and M are angular momentum and mass parameter of the black hole respectively, and E and J_z are given as energy and momentum per mass of the particle. In the above, we assume $(0,1,2,3)$ are (t, r, θ, ϕ) respectively. The expressions for P_s and Σ_s are given as

$$P_s = E\left(r^2 + a^2 + aS + \frac{aSM}{r}\right) - \left(a + \frac{MS}{r}\right) J_z,$$

$$\Sigma_s = r^2(1 - MS^2/r^3); \qquad \Delta = r^2 + a^2 - 2Mr,$$

$$\Lambda_s = 1 - \frac{3MS^2 r}{\Sigma_s^3}\{J_z - (a + S)E\}^2. \qquad (6)$$

For $S > 0$, the spin is parallel to the z axis, and antiparallel for $S < 0$. In addition, to guarantee that the timelike constraint $\mathcal{U}^i \mathcal{U}_i < 0$ is always valid, we have the following condition to hold:

$$r^5(1 - MS^2/r^3)^4$$
$$- 3MS^2(2 + MS^2/r^3)\{J_z - E(a + S)\}^2 > 0. \quad (7)$$

Needless to say, the above condition further constrains the motion of the particle, and, especially close to the horizon, it becomes more dominant [35].

III. RESONANCE PHENOMENON AND FUNDAMENTAL FREQUENCIES

The general condition for resonance can be written in terms of the fundamental frequencies, such that

$$\alpha\Omega_r + \beta\Omega_\theta + \gamma\Omega_\phi = 0, \qquad (8)$$

where α, β, and γ are rational numbers without any common divisors. For a limiting case on the equatorial plane, Ω_r and Ω_ϕ would be of particular interest, while Ω_θ has no meaning. On the other hand, for circular orbits, Ω_r is not particularly relevant and Ω_θ and Ω_ϕ play the key role in the orbital dynamics. In the present context, we shall be interested in following investigations:

(i) The quasiperiodic oscillations for spinning particles and the locations of resonant orbits from the condition given by Eq. (8).

(ii) Location of resonant orbits on the equatorial plane following the condition $\alpha\Omega_r + \gamma\Omega_\phi = 0$ which is the $r\phi$ resonance.

In the first case, we consider that the particle is following a nearly circular orbit, and also executing small oscillation about the equatorial plane. The detailed calculations to obtain the fundamental frequencies are given by Hinderer *et al.* in Ref. [63], and we explicitly employ them in our purpose. We study the resonance phenomenon related to these frequencies in Sec. IV. However, as already mentioned, the present analysis is valid only at $\mathcal{O}(S)$, i.e., $|S| \ll 1$, which is exactly the appropriate regime to describe an extreme mass ratio system through the Mathisson-Papapetrou equations [24].

In the case of a generic elliptical orbit, we may introduce the following expressions for radial and azimuthal frequencies:

$$\Omega_r = \frac{2\pi}{T_r}, \quad \text{and} \quad \Omega_\phi = \frac{\Delta\phi}{T_r}, \tag{9}$$

where $T_r = 2\int_{r_a}^{r_p}\left(\frac{dt}{dr}\right)dr$ and $\Delta\phi = 2\int_{r_a}^{r_p}\left(\frac{d\phi}{dr}\right)dr$, and r_a and r_p are the apastron and periastron radii respectively [64,65]. In this case, the $r\phi$ resonance would be governed by the equation

$$m\Omega_r - n\Omega_\phi = 0, \tag{10}$$

where m and n are two integers constrained as $n \le m$. More conveniently, the above equation can be written as

$$m\pi - n\int_{r_p}^{r_a}\frac{d\phi}{dr}dr = 0. \tag{11}$$

The second term in the above expression can be written as

$$\frac{d\phi}{dr} = \left(\frac{d\phi}{d\tau}\right)\left(\frac{dr}{d\tau}\right)^{-1}, \tag{12}$$

with τ being the proper time. By comparing with the parametrization given in Sec. II, there seems to exist an apparent contradiction. However, it can be further explained as follows: given that the parametrization $P^i\mathcal{U}_i = -\mu$ is valid, the affine parameter is given by σ—which may not be the proper time. Therefore, $\mathcal{U}^i$ is a tangent to the curve, but not the four velocity. In particular, the Mathisson-Papapetrou equations can now be written as

$$\frac{DP^a}{d\sigma} = -\frac{1}{2}R^a_{bcd}\left(\frac{dx^b}{d\sigma}\right)S^{cd},$$
$$\frac{DS^{ab}}{d\sigma} = P^a\left(\frac{dx^b}{d\sigma}\right) - P^b\left(\frac{dx^a}{d\sigma}\right). \tag{13}$$

However, with the relation

$$\frac{d}{d\sigma} = \frac{d\tau}{d\sigma}\frac{d}{d\tau} \tag{14}$$

being introduced, the above equation can be casted again as Eq. (2), provided that $(d\tau/d\sigma)$ is nonzero. Therefore, the time parametrization given in Sec. II can be employed to describe usual dynamics of a spinning particle. Moreover, in the present context, we have only considered terms up to linear order in spin, and therefore, the parametrization with respect to both τ and σ would have the same result. Coming back to Eq. (12), it can be further simplified by introducing the orbit equations in terms of energy, angular momentum, spin, and the radial coordinate r. However, it is evident that the quantity $dr/d\tau$ is proportional to the radial potential, which in fact vanishes at the turning points r_a and r_p. This constitutes a serious problem while integrating the function that blows up in the upper and lower limits. We shall use approximate technique, namely the Sochnov method, to deal with such scenarios.

IV. NEARLY CIRCULAR AND EQUATORIAL ORBITS AND RESONANCE CONDITIONS

Let us now consider the nearly circular and equatorial orbits for spinning particles and determine the small oscillation frequencies accordingly. For this purpose we shall assume the spin vector has the form $S = (0, 0, S^\theta, 0)$ and the four velocity can be written as $\mathcal{U}^i = (\mathcal{U}^0, 0, 0, \mathcal{U}^3)$. In addition, we shall approximately write the frequencies up to the linear order in spin while neglecting all the higher order terms.

A. Fundamental frequencies Ω_r, Ω_θ, and Ω_ϕ

We now introduce the fundamental frequencies as given in Ref. [63]. Given that we are only considering the terms linear in spin, the frequencies for both corotating and counterrotating orbits take the following form:

$$\frac{\Omega_r^2}{\Omega_\phi^2} = \frac{(r_c - 6M)r_c - 3a^2 \pm 8a\sqrt{Mr_c}}{r_c^2} + \frac{6S(\pm\sqrt{Mr_c} - a)[(r_c - 3M)\sqrt{r_c} \pm 2a\sqrt{M}]}{r_c^{7/2}} + \mathcal{O}(S^2), \tag{15}$$

$$\frac{\Omega_\phi}{\Omega_\theta} = \frac{r_c}{\sqrt{3a^2 \mp 4a\sqrt{Mr_c} + r_c^2}} - \frac{3aS\{\pm 2a\sqrt{M} + (r_c - 3M)\sqrt{r_c}\}}{\sqrt{r_c}\{3a^2 \mp 4a\sqrt{Mr_c} + r_c^2\}^{3/2}} + \mathcal{O}(S^2), \tag{16}$$

$$\Omega_\phi = \frac{\sqrt{M}}{r_c^{3/2} \pm a\sqrt{M}}, \tag{17}$$

where r_c is the radius of the circular orbit about which the spinning particle is executing small oscillation and upper and lower sign corresponds to corotating and counter-rotating orbits respectively. In the next section, we employ the above frequencies to obtain the resonant orbits for a spinning particle.

B. Locations of the resonant orbits

Having described various frequencies corresponding to the small oscillation of a spinning particle, we can now demonstrate the resonant orbits depending on their spin parameters and a black hole's angular momentum. In Fig. 1, the corotating resonant orbits are depicted as a
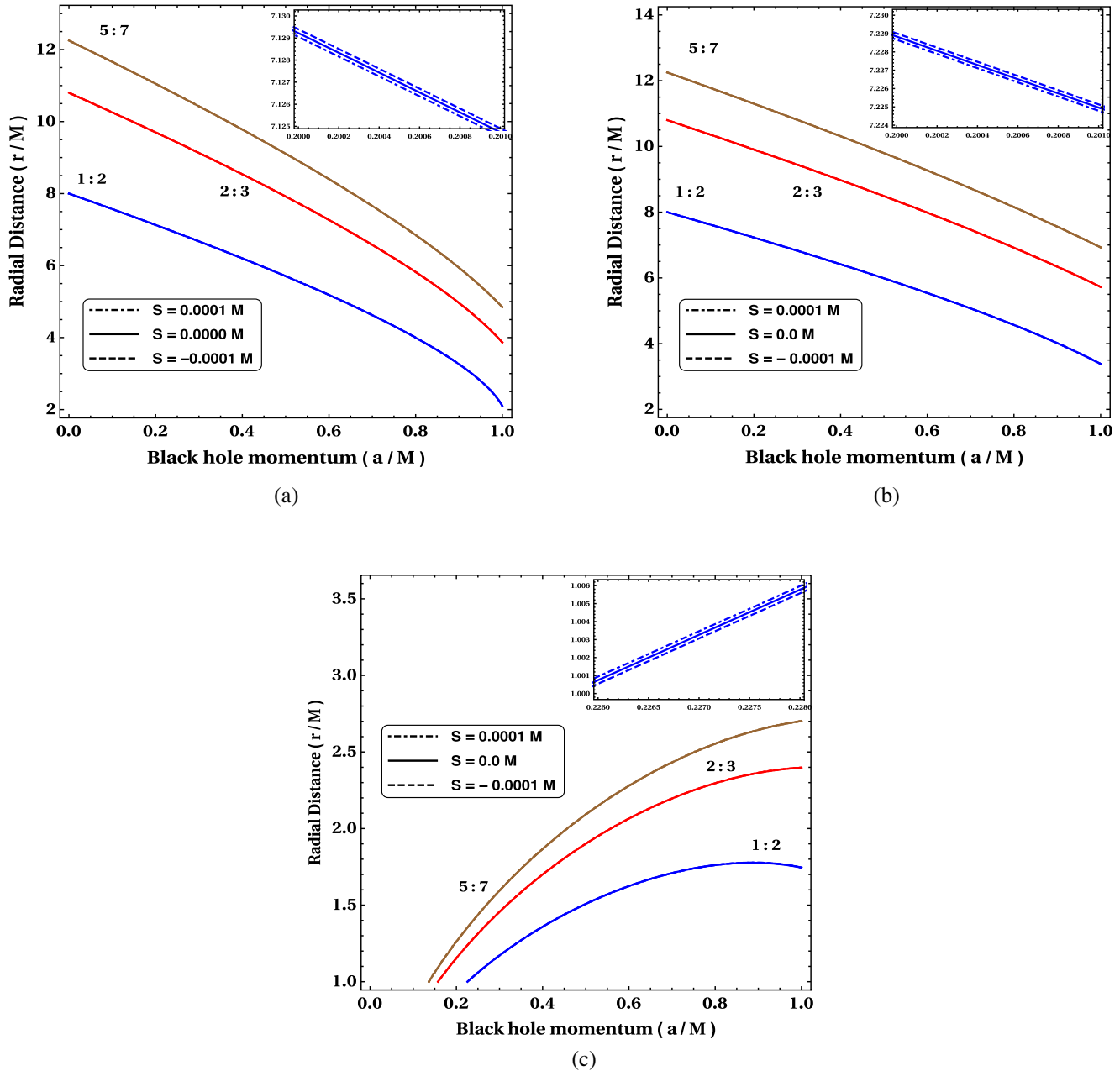

FIG. 1. Location of corotating resonant orbits for different spin parameters and a black hole's momentum. Here, we have used Eqs. (15), (16), and (17) to obtain images. Distinguishing features related to various resonances are also depicted for different orders. The blue, red, and brown colors are related to 1∶2, 2∶3, and 5∶7 resonance order respectively. In the inset of each plot, we have plotted the closeup curve for 1∶2 resonance. (a) $r\theta$ resonant orbits are shown as a function of the black hole's momentum while the spin of the particle takes different values. (b) $r\phi$ resonance for different spins of the extended object. (c) $\theta\phi$ resonance is depicted as a function of the black hole's momentum.

function of the black hole's momentum while the spin parameter takes different values. The significance of the resonant orders are also demonstrated for $r\theta$, $r\phi$, and $\theta\phi$ resonances in Figs. 1(a)–1(c) respectively. Given a larger order, the orbits move away from the horizon and as it is shown in Fig. 1, this is true for each of the resonance frequencies. Furthermore, it should also be emphasized that both $r\theta$ and $r\phi$ follow an identical behavior while the $\theta\phi$ consists with a stark contrast from them. While in case of the $r\theta$ and $r\phi$ resonances, the orbits begin to move closer to

the event horizon as one increases the black hole's momentum, nearly opposite phenomena happens for $\theta\phi$. This is related to the fact that a larger momentum of the black hole drags the prograde orbits close to its horizon while the opposite is true for retrograde orbits. Because of the presence of r in both $r\theta$ and $r\phi$ resonances, this nature is largely influential in either of these cases. But in case of $\theta\phi$ resonance, this is no longer valid and the orbits behaves quite differently from $r\theta$ and $\theta\phi$ resonances. Similarly, the resonant orbits for the counterrotating trajectories are given
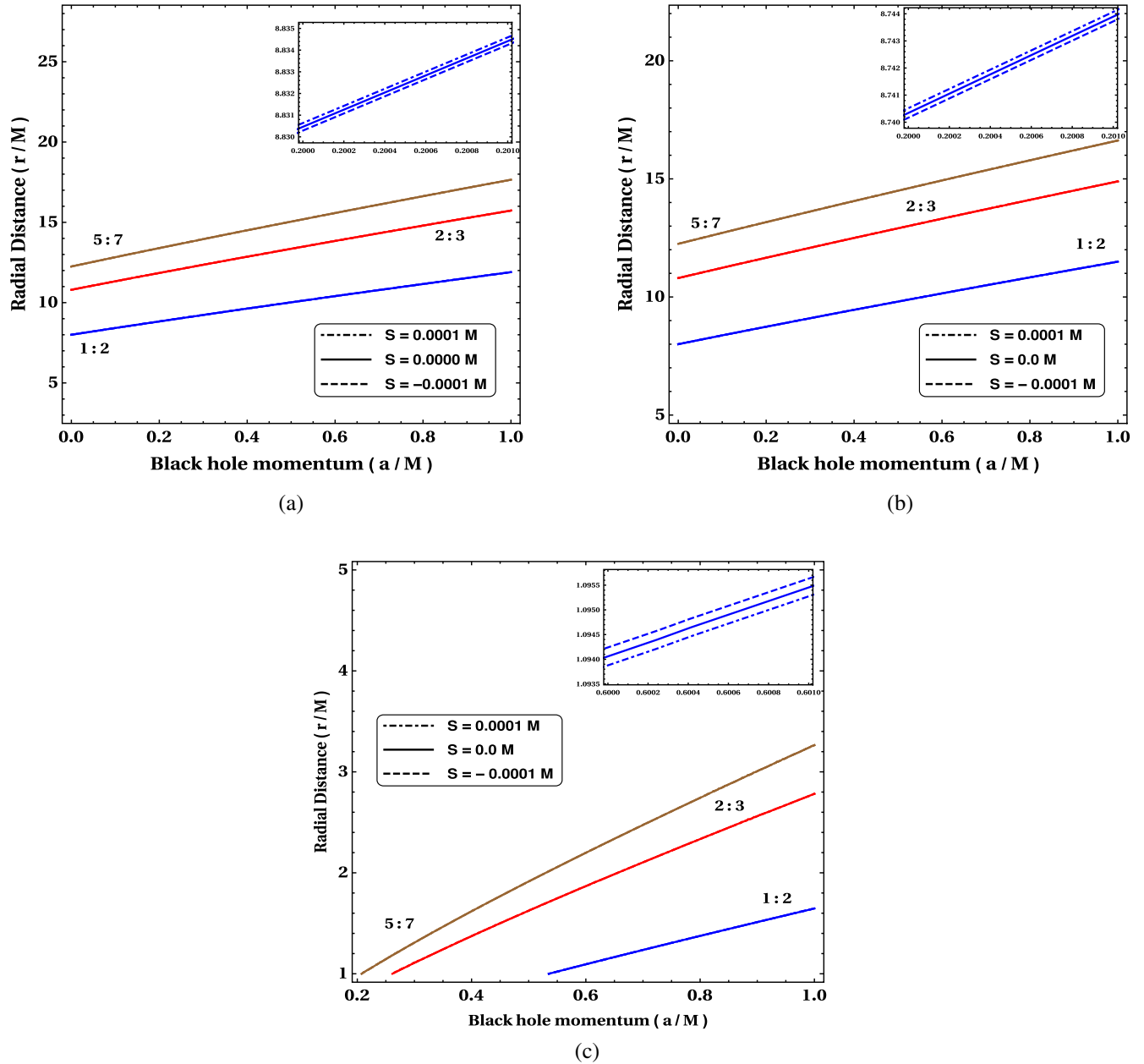

FIG. 2.   Counterrotating resonant orbits as a function of the black hole's angular momentum and different spin of the extended object. As expected, with the increase of the black hole's momentum, the orbits move away from the horizon. (a) $r\theta$ resonance in counterrotating orbits for different spin parameters. (b) $r\phi$ resonance as a function of the black hole's angular momentum. (c) $\phi\theta$ resonant orbits for different spins of the secondary object.

in Fig. 2. Interestingly, $\theta\phi$ resonance has now becomes $\phi\theta$. Mathematically, this is straightforward to understand from the relation given in Eq. (16), which stands as follows for the spinless case:

$$\frac{\Omega_\phi}{\Omega_\theta} = \frac{r_c}{\sqrt{3a^2 \mp 4a\sqrt{Mr_c} + r_c^2}}. \qquad (18)$$

For the upper sign or corotating case, it is possible to find $\Omega_\theta < \Omega_\phi$, while in the counterrotating case, Ω_θ is always greater than Ω_ϕ. Therefore, in order to retain the convention used in Eq. (11), we employ $\phi\theta$ resonance for the counterrotating case. In the case of a spinning particle within the linear approximation, the above explanation remains the same.

With this, we finish our discussions regarding the resonance phenomenon between the small oscillations frequencies for a spinning particle with its spin approximated up to the linear order term. In the upcoming section, we consider the $r\phi$ resonance corresponding to a generic trajectory confined on the equatorial plane of a Kerr black hole.

V. MOTION ON THE EQUATORIAL PLANE: THE $r\phi$ RESONANCE

With the introduction to resonant orbits for a spinning particle orbiting in nearly circular trajectories close to the equatorial plane, we grasp the basic mechanism to locate them as a function of the radial distance r. However, to address any general motion it is presumed that orbits are neither nearly circular nor close to the equatorial plane and a universal prescription is required to study them. In the case of geodesics, these are well studied in literature since Carter discovered the existence of a fourth conserved quantity and concluded that the geodesic trajectories are completely integrable in the Kerr background [43]. However, in the case of a spinning particle, general off-equatorial orbits can be nontrivial to obtain; recent studies on these aspects can be found in Refs. [46,47]. Nonetheless for orbits confined on the equatorial plane, the Mathisson-Papapetrou equations can be exactly solved and thereby the resonance between the radial Ω_r and azimuthal Ω_ϕ frequency can be well determined. The primary equation governing this resonance phenomena is given as $m\Omega_r - n\Omega_\phi = 0$ and stated in Eq. (11). From the solutions of Mathisson-Papapetrou equations, we can express $\frac{d\phi}{dr}$ as

$$\frac{d\phi}{dr} = \frac{\mathcal{U}^3}{\mathcal{U}^1} = \frac{1}{\sqrt{R_s}}\left[\left(1 + \frac{3MS^2}{r\Sigma_s}\right)\{J_z - (a+S)E\} + \frac{a}{\Delta}P_s\right], \qquad (19)$$

where $\mathcal{U}^1$ and $\mathcal{U}^3$ are radial and azimuthal velocity respectively and the quantities P_s, R_s, Σ_s have been defined in Eq. (6).

In the upcoming sections, we shall explicitly employ the above expression to locate the $r\phi$ resonance orbits in both Schwarzschild and Kerr geometries. However before studying any resonance phenomena, it is advisable to notice that the radial velocity $\mathcal{U}^1$ identically vanishes in the turning points (r_a, r_p) and as a result the integral in Eq. (11) would diverge. Therefore to compute the integral we may use an approximate technique and in the present context, Sochnev method can be extremely useful [66] (we also refer to Ref. [65] where this is used in the case of a spinning particle). For convenience, the basic design of the Sochnev method is given below.

Let us consider an irrational function given as

$$C = \sqrt{C_1 C_2 \dots C_m} \qquad (20)$$

and we desire to approximate it for our convenience. In the above, $C_1, C_2, \dots C_m$ are positive numbers. The first step of the Sochnev method [66] dictates that the value of C would fall within the upper limit a_1 and lower limit b_1 which are given by the following expressions:

$$a_1 = \frac{C_1 + C_2 + \cdots \dots C_m}{2}, \qquad b_1 = \frac{C_1 C_2 \dots C_m}{a_1^{m-1}},$$
$$\text{and} \quad b_1 < C < a_1, \qquad (21)$$

while more accuracy can be achieved with next order terms. The final expression of the sequence (a_n, b_n) can be written as

$$a_{n+1} = \frac{(m-1)a_n + b_n}{m}, \qquad b_{n+1} = \frac{(a_n)^{m-1}b_n}{(a_{n+1})^{m-1}}, \qquad (22)$$

and for large n, it is expected both a_n and b_n would generate extremely accurate values of C. However, in the present context we often neglect the higher order n terms and truncate our series at (a_1, b_1). Due to the nonzero spin terms the expressions become largely cumbersome to probe higher order terms with $n > 1$.

A. In the Schwarzschild black hole

Let us now describe the $r\phi$ resonance in the static and spherically symmetric Schwarzschild black hole and later on we discuss the Kerr geometry. For convenience, we start with the geodesic trajectories and then address the motion of a spinning particle.

1. Geodesic limit

Due to the spherical symmetry, geodesic trajectories in Schwarzschild spacetime are vastly simplified and easily obtainable in comparison to the rotating case. To study the resonance phenomena in the Schwarzschild background, we set $\theta = \pi/2$ without losing any generality and obtain the radial potential as follows:

$$r^4(\mathcal{U}^1)^2 = V(r) = E^2 r^4 - r^2 L_z^2 + 2MrL_z^2 - (r^2 - 2Mr)r^2, \tag{23}$$

where E and L_z are given as the conserved energy and momentum associated with the timelike and spacelike symmetries of the geometry respectively. As we mentioned earlier, at $r = r_a$ and $r = r_p$ the radial potential identically vanishes, i.e., $V(r_a) = V(r_p) = 0$, and we can arrive at the expressions for E and L_z in terms of r_a and r_p. These are given by

$$E_{\text{geo}}^2 = \frac{(r_a + r_p)(2M - r_a)(2M - r_p)}{r_a r_p(r_a + r_p) - 2M(r_a^2 + r_p^2 + r_a r_p)} \quad \text{and} \quad L_{z\text{geo}}^2 = \frac{2Mr_a^2 r_p^2}{r_a r_p(r_a + r_p) - 2M(r_a^2 + r_p^2 + r_a r_p)}. \tag{24}$$

Substituting these expression in the potential given by Eq. (23) we arrive at

$$V(r) = -\frac{2M(r - r_a)(r - r_p)(r - 0)(r - r_c)\{r_a r_p - 2M(r_a + r_p)\}}{r_a r_p(r_a + r_p) - 2M(r_a^2 + r_p^2 + r_a r_p)}, \tag{25}$$

where we have $r_c = \frac{2Mr_a r_p}{r_a r_p - 2M(r_a + r_p)}$ and the solutions follow $r_a > r_p > r_c$. From the expression, $r_p > r_c$, we arrive at

$$\frac{p - 4M}{2M(1 + e)} > 1 \Rightarrow p > 2M(3 + e). \tag{26}$$

Furthermore, with the expressions for square of momentum given in Eq. (24), we require $L_{z\text{geo}}^2 > 0$. Therefore from the denominator, we gather

$$r_a r_p(r_a + r_p) > 2M(r_a^2 + r_p^2 + r_a r_p), \tag{27}$$

and from Eq. (25), we arrive at

$$(r - r_a)(r - r_p)(r - r_c)\{r_a r_p - 2M(r_a + r_p)\} < 0. \tag{28}$$

By using Eq. (26), one can establish $r_a r_p - 2M(r_a + r_p) > 0$, and the above equation is automatically satisfied. Moreover, Eq. (27) can be further simplified by using $r_a = p/(1 - e)$ and $r_p = p/(1 + e)$, and we arrive at

$$\frac{2p^2[p - M(3 + e^2)]}{(1 - e^2)^2} > 0, \tag{29}$$

and for $p > M(3 + e^2)$, it is always satisfied. Therefore, the final constraint on the semilatus varies between $p = 6M$ (for circular orbit) and $p = 8M$ (highest eccentric orbit $e = 1$).

2. Spinning particle

For a nonvanishing spin of the particle, the rescaled potential can be written as

$$V_s(r) = r^4 R_s = r^4[(E^2 - 1)r^4 + 2Mr^3 - r^2 J_z^2 + 2rJ_z\{MJ_z + ES(r - 3M)\}], \tag{30}$$

and by setting $S = 0$, we get back the potential for a geodesic. Furthermore, it should be emphasized that the above equation contains terms only linear in S while the higher order terms are ignored for a convenient computation. Naturally, one could ask whether the above potential gives the correct location for circular orbits or not. This could be easily verified as we already have the exact expression for radial potential for a spinning particle, given in Eqs. (5) and (6). It can be shown that within the small spin approximation, i.e., $|S| \ll 1$, the above potential provides the locations of circular orbits within an infinitesimal mismatch from the exact derivation. For example, given a spin of $S = 0.1M$ and energy $E = 1$, the location of the circular orbits mismatch within $\mathcal{O}(10^{-3})$. With that spirit, we employ the above linearized expression and it simplifies our computations. We shall now concentrate on obtaining the expressions for energy and momentum assuming an ansatz of the form $E_{\text{sbh}} = E_{\text{geo}} + SE_s$ and $J_{\text{sbh}} = L_{z\text{geo}} + SJ_s$ is valid. With the prior knowledge about both E_{geo} and L_{geo} [67], we can solve $V_s(r_a) = V_s(r_p) = 0$ and obtain E_s and J_s in terms of r_a and r_p. Both E and J_s are given as follows:

$$J_s = \frac{\sqrt{(2M - r_a)(2M - r_p)(r_a + r_p)}[r_a r_p(r_a + r_p) - 3M(r_a^2 + r_a r_p + r_p^2)]}{[r_a r_p(r_a + r_p) - 2M(r_a^2 + r_a r_p + r_p^2)]^{3/2}},$$

$$E_s = \frac{-M\sqrt{2M}r_a r_p}{[r_a r_p(r_a + r_p) - 2M(r_a^2 + r_a r_p + r_p^2)]^{3/2}}. \tag{31}$$

Further employing the above relations into the potential given up to the linear order in spin, we arrive at

$$V_s(r) = \frac{2Mr^5 a_0(r - r_a)(r - r_p)}{[r_a r_p(r_a + r_p) - 2M(r_a^2 + r_p^2 + r_a r_p)]^2}\left[r + \frac{b_0}{a_0}\right],$$ (32)

where a_0 and b_0 are given by

$$\begin{aligned}
a_0 &= -[r_a r_p - 2M(r_a + r_p)]\{r_a r_p(r_a + r_p) - 2M(r_a^2 + r_p^2 + r_a r_p)\} \\
&\quad - Sr_a r_p\{2M(r_a - 2M)(r_p - 2M)(r_a + r_p)\}^{1/2}, \\
b_0 &= 2Mr_a r_p\{r_a r_p(r_a + r_p) - 2M(r_a^2 + r_p^2 + r_a r_p)\} \\
&\quad - Sr_a r_p(r_a + r_p)\{2M(r_a - 2M)(r_p - 2M)(r_a + r_p)\}^{1/2}.
\end{aligned}$$ (33)

It should be noted that even if the number of solutions remains identical with the geodesic case, there now exists explicit spin dependence in one of the solutions $r_s = -b_0(a_0)^{-1}$. Finally, the potential can be compactly written in the form of

$$V_r(s) = \frac{2Ma_0 r^4(r - 0)(r - r_a)(r - r_p)(r - r_s)}{[r_a r_p(r_a + r_p) - 2M(r_a^2 + r_p^2 + r_a r_p)]^2},$$ (34)

and identical to the geodesic case, we require to have $V_r(s) > 0$. This condition along with the bound $r_p < r < r_a$ would give $r_p > r_s$ and $a_0 < 0$. However, either of these constraints would depend on the numerical value of the spin parameter and therefore while obtaining the resonant orbits, we will employ it explicitly.

With the above mentioned points kept in mind, we now determine $\mathcal{U}^3(\mathcal{U}^1)^{-1}$ from Eq. (19) and in the linear spin approximation, this is given as

$$\frac{d\phi}{dr} = \frac{(J_z - ES)\{r_a r_p(r_a + r_p) - 2M(r_a^2 + r_p^2 + r_a r_p)\}}{[2Ma_0(r - 0)(r - r_a)(r - r_p)(r - r_s)]^{1/2}}.$$ (35)

By substituting it in Eq. (11), we arrive at the following expression which describes the $r\phi$ resonance for a given particle:

$$m\pi - n\int_{r_p}^{r_a}\left(\frac{d\phi}{dr}\right)dr = m\pi - nI_s = 0.$$ (36)

In the discussions given below, we employ the Sochenev formalism that was earlier introduced in Sec. V and compute I_s approximately. However for a convenient and simplified computation, we confine our discussions only with the first order approximation, i.e., we assume $(C_1 C_2)^{1/2} \approx 2^{-1}(C_1 + C_2)$ is valid throughout our calculations.

In order to obtain an approximate value for the above integral, we start with

$$\int_{r_p}^{r_a}\frac{d\phi}{dr}dr = N\int_{r_p}^{r_a}\frac{dr}{\sqrt{a_0(r - 0)(r - r_a)(r - r_p)(r - r_s)}},$$ (37)

where $N = (2M)^{-1/2}(J_z - ES)\{r_a r_p(r_a + r_p) - 2M(r_a^2 + r_p^2 + r_a r_p)\}$ and a_0 is already defined earlier. Let us now introduce a coordinate transformation given as $r = 2^{-1}[(r_a + r_p) + x(r_a - r_p)]$ and with that, we arrive at

$$I_s = \int_{r_p}^{r_a}\left(\frac{d\phi}{dr}\right)dr = \int_{-1}^{1}\left(\frac{d\phi}{dx}\right)dx.$$ (38)

Finally we have

$$\begin{aligned}
\frac{d\phi}{dx} &= \frac{r_a - r_p}{2}\frac{d\phi}{dr} \\
&= \frac{r_a - r_p}{2}\frac{N}{\{-a_0\frac{(r_a - r_p)^2}{4}(1 - x^2)(r - 0)(r - r_s)\}^{1/2}},
\end{aligned}$$ (39)

and after further simplification, we write it as follows:

$$\frac{d\phi}{dx} = \frac{N}{\{-a_0(1 - x^2)(r - 0)(r - r_s)\}^{1/2}},$$ (40)

$$\begin{aligned}
&= N\{-a_0\frac{(r_a + r_p)}{2}\frac{(r_a + r_p - 2r_s)}{2} \\
&\quad \times (1 - x^2)(1 + K_0 x)(1 + K_s x)\}^{-1/2}.
\end{aligned}$$ (41)

With $\langle N\rangle$ given by

$$\langle N\rangle = 2N\{-a_0(r_a + r_p)(r_a + r_p - 2r_s)\}^{-1/2},$$ (42)

the above can be written in a more compact form as

$$\frac{d\phi}{dx} = \frac{\langle N\rangle}{\{(1 - x^2)(1 + K_0 x)(1 + K_s x)\}^{1/2}},$$ (43)
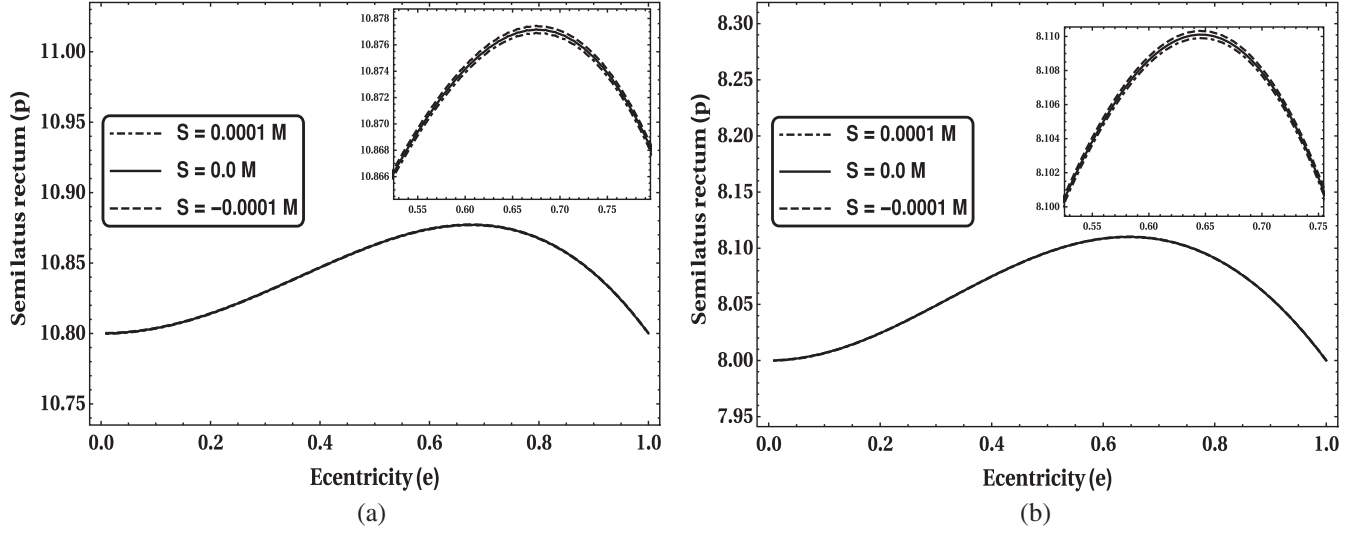
FIG. 3.   Various $r\phi$ resonant orbits in a Schwarzschild spacetime for both spinning and nonspinning trajectories. In the inset, we show a closeup of a particular segment to show the difference for various spin parameters. (a) Orbits for 2:3 resonance is given for both spinning and nonspinning particles. For a negative spin parameter of the particle, the resonant orbits appear at a larger range of p while for positive spin the opposite phenomenon appears. (b) Orbits for 1:2 resonance are given in a Schwarzschild back- ground. The distinguishing features for both positive and negative values of spin are given explicitly.

where we have, $K_0 = \frac{r_a - r_p}{r_a + r_p}$ and $K_s = \frac{r_a - r_p}{r_a + r_p - 2r_s}$. Furthermore, to ease our computations, we introduce the expression

$$\int_{-1}^{1} \frac{1}{\sqrt{1 - x^2}(1 + Kx)} dx = \frac{\pi}{\sqrt{1 - K^2}}, \qquad (44)$$

which is only valid with $K < 1$. We can use the same technique in our case by writing $\sqrt{(1 + K_0 x)(1 + K_s x)} \approx (1 + \frac{K_0 + K_s}{2}) = 1 + Kx$ and therefore, the final expression becomes

$$I_s = \int_{-1}^{1} \frac{d\phi}{dx} dx = \frac{\pi \langle N \rangle}{\sqrt{1 - K^2}}. \qquad (45)$$

With the above relation and by using Eq. (36), the resonance condition takes the form

$$m - n \frac{\langle N \rangle}{\sqrt{1 - K^2}} = 0. \qquad (46)$$

We shall now employ the above condition and locate the resonant orbits for a spinning particle moving around a Schwarzschild black hole. In Fig. 3, we demonstrate the same for both 2:3 [Fig. 3(a)] as well as 1:2 [Fig. 3(b)] resonance condition.

B. In the Kerr black hole

Having described the resonance phenomena in Schwarzschild background, we shall continue our discussions in the Kerr spacetime and as expected, in rotating geometry the motion of a spinning particle is additionally complicated. Therefore before delving into the details of a spinning particle, we start with the geodesic case and then address the extended object in both linearized Kerr and full Kerr spacetime.

1. Geodesic limit

To locate the resonant orbits for a geodesic, we need to employ the following relation:

$$\frac{d\phi}{dr} = \frac{\mathcal{U}^3}{\mathcal{U}^1}$$

$$= \frac{r^2 \{L_z - aE + \frac{a}{\Delta}[E(r^2 + a^2) - aL_z]\}}{\{r^4[E(r^2 + a^2) - aL_z]^2 - \Delta[r^6 + (L_z - aE)^2 r^4]\}^{1/2}}, \qquad (47)$$

in Eq. (11). With a more simplified form, the above can be written as

$$\frac{d\phi}{dr} = \frac{\{L_z - aE + \frac{a}{\Delta}[E(r^2 + a^2) - aL_z]\}}{\{[E(r^2 + a^2) - aL_z]^2 - \Delta[r^2 + (L_z - aE)^2]\}^{1/2}}$$

$$= \frac{\{L_z - aE + \frac{a}{\Delta}[E(r^2 + a^2) - aL_z]\}}{\{V(r)\}^{1/2}}, \qquad (48)$$

and the potential takes the form

$$V(r) = [E(r^2 + a^2) - aL_z]^2 - \Delta[r^2 + (L_z - aE)^2]. \qquad (49)$$

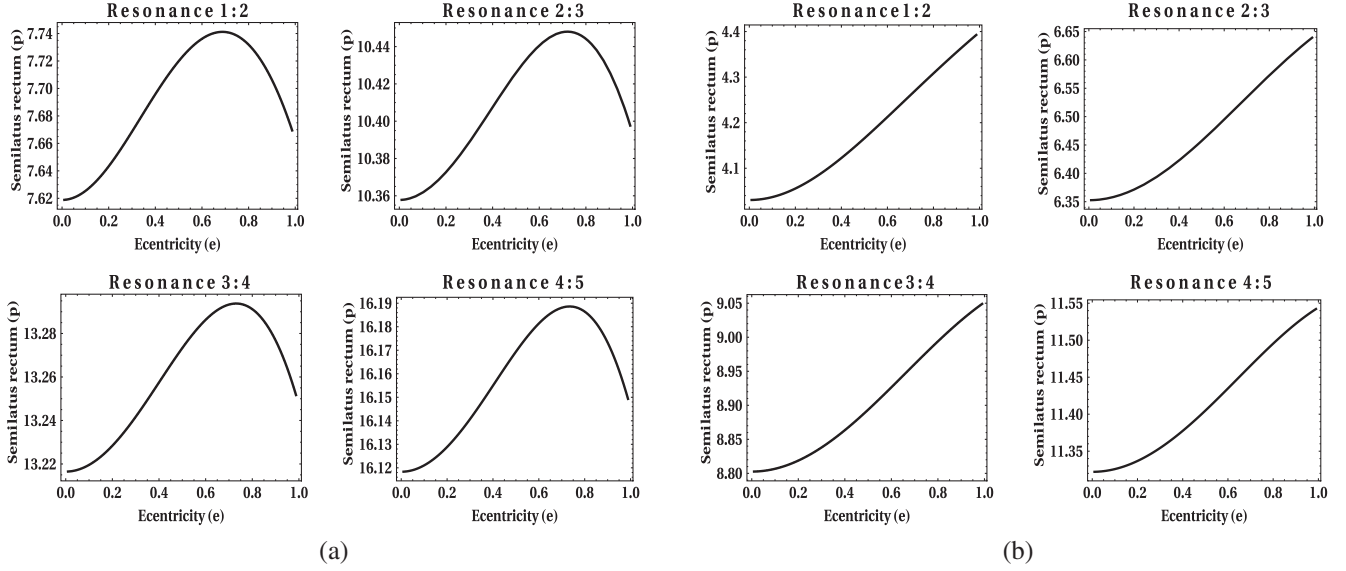By further simplification, we arrive at

FIG. 4. Various $r\phi$ resonant orbits in the Kerr spacetime for nonspinning trajectories. (a) Resonant orbits are given for $a = 0.1M$. With the increase in eccentricity, the semilatus rectum increases and reaches a maximum value at $p = p^{\max}$ while further increase in eccentricity decreases p as well. (b) Resonant orbits for a geodesic while the background is given by a Kerr geometry with $a = 0.9M$. The nature of the plot changes drastically from (a).

$$V(r) = r[E^2r^3 - (L_z^2 - a^2E^2)r + 2M(L_z - aE)^2$$
$$- (r^2 - 2Mr + a^2)r]$$
$$= -\alpha(r - 0)(r - r_a)(r - r_p)(r - r_1), \qquad (50)$$

with $\alpha = 1 - E^2$. From the above equation, we can now match the coefficients of r^3, r^2, and r from each side. These would reproduce three independent equations and we can solve for energy, momentum, and r_1 in terms of r_a and r_p. Finally, we have

$$E^2 = 1 - \frac{2M}{r_a + r_p + r_1} \quad \text{and}$$

$$L_z^2 = \frac{2M}{r_a + r_p + r_1}\{r_a r_p + r_1(r_a + r_p) - a^2\}, \qquad (51)$$

and the solution r_1 can be evaluated from the other condition

$$4aMEL_z = 2Ma^2E^2 + 2ML_z^2 - (1 - E^2)r_1 r_a r_p. \qquad (52)$$

By solving the above equation numerically for a given eccentricity e and semilatus rectum p, we obtain r_1 and therefore, determine both energy and momentum corresponding to the orbit. Henceforth, for any provided r_a and r_p we can obtain the conserved quantities required to specify the geodesic trajectory. The reader should be reminded that Eq. (52) is a quadratic of r_1 and these two solutions represent either prograde or retrograde orbits. Like we mentioned earlier, as we are interested in the prograde orbit, we would suppress the retrograde part and continue our analysis with that motivation. Nonetheless, a similar

study can be carried out in the case of retrograde orbits too. The next task is to compute the integral given in Eq. (11) and locate the resonant orbits for an arbitrary order and this is carried out in the Appendix for both spinning and nonspinning trajectories. In Fig. 4, we have shown the resonant orbits for a geodesic moving in a spacetime with different rotation parameters a. For smaller values of a, the resonant orbits lie away from the black hole horizon and the nature remains similar to the Schwarzschild case. With the increase of resonance order, i.e., $m + n$, the orbits keep moving away from the horizon but are contained with identical properties as given in Fig. 4(a). However for larger momentum, the peak seems to disappear and the Gaussian nature changes to linear curve. This is explicitly shown in Fig. 4(b).

2. Spinning particle: In the slowly rotating Kerr black hole

With the discussions presented above for geodesic trajectories, we shall now consider the case with spinning particles and locate their resonance orbits. However before dealing with the Kerr spacetime that consists with the multipole structure of arbitrary order, we first consider only the dipole current moment and approach it analytically to obtain the expressions for energy and momentum. In the usual Boyer-Lindquist coordinates, the resultant metric takes the following form:

$$ds^2 = -\left(1 - \frac{2M}{r}\right)dt^2 + \left(1 - \frac{2M}{r}\right)^{-1}dr^2$$
$$+ r^2(d\theta^2 + \sin^2\theta d\phi^2) - \frac{4Ma\sin^2\theta}{r}d\phi dt, \qquad (53)$$

with a and M given as the angular momentum per mass and mass of the spacetime respectively. For the above metric, we obtain the radial potential written up to the terms linear in S as

$$V_s(r) = r^3[r\{E^2 r^4 - J_z^2 r^2 + 2MrJ_z^2 - 4aMrEJ_z - (r^2 - 2Mr)r^2\}$$
$$+ S(2EJ_z r^3 - 6EMJ_z r^2 + 2aMJ_z^2 + 6MaE^2 r^2)], \tag{54}$$

and after further simplifications, we arrive at the following expression:

$$V_s(r) = r^3[r\{(E^2 - 1)r^4 + 2Mr^3 - r^2 J_z^2 + 2r(MJ_z^2 + EJ_z S(r - 3M) + 3aME^2 S - 2aMEJ_z)\} + 2aMSJ_z^2]. \tag{55}$$

We shall now assume $E = E_{sbh} + aE_s$ and $J_z = J_{sbh} + aJ_s$ and solve for E_s and J_s from the equations $V_s(r_a) = V_s(r_p) = 0$. Such assumptions would ensure that only the terms linear to a are considered, while higher order terms, i.e., $\mathcal{O}(a^2)$ and beyond, are neglected. In order to deal with larger momentum of the black hole, we carry out a numerical analysis in the next section. Due to the complexity of the forms of both E_s and J_s, they are not explicitly written in the present paper. By substituting them in Eq. (55), we can write down the potential $V_s(r)$ as

$$V_s(r) = r^3[V_s^{sbh}(r) + aV_s^{kerr}(r)], \tag{56}$$

where $V_s^{sbh}(r)$ and $V_s^{kerr}(r)$ can be written as

$$V_s^{sbh}(r) = \frac{2Mr^2(r - r_a)(r - r_p)}{\mathcal{X}^3}[\mathcal{X}^2(2M\{r_a r_p + r(r_a + r_p)\} - rr_a r_p) - r_a r_p(r + r_a + r_p)\mathcal{Y}^{1/2}\mathcal{X}S],$$
$$V_s^{kerr}(r) = \frac{2M(r - r_a)(r - r_p)F(r)}{\mathcal{X}^3}, \tag{57}$$

and $F(r)$, $\mathcal{X}$, and $\mathcal{Y}$ have the following expressions:

$$F(r) = -2r^2 r_a r_p \mathcal{X}\mathcal{Y}(r + r_a + r_p) + r^2[(2M\{r_a r_p + r(r_a + r_p)\} - rr_a r_p)\mathcal{X}^2 - r_a r_p(r + r_a + r_p)\mathcal{X}\mathcal{Y}S],$$
$$\mathcal{X} = r_a r_p(r_a + r_p) - 2M(r_a^2 + r_a r_p + r_p^2), \mathcal{Y} = 2M(2M - r_a)(2M - r_p)(r_a + r_p). \tag{58}$$

Therefore, the complete form of the potential can be written as

$$V_s(r) = \frac{2Mr^3(r - r_a)(r - r_p)}{\mathcal{X}^3}[F(r) + r^2\mathcal{X}^2(2M\{r_a r_p + r(r_a + r_p)\}) - r^2 r_a r_p(r + r_a + r_p)\mathcal{Y}^{1/2}\mathcal{X}S],$$
$$= \frac{2Mr^3(r - r_a)(r - r_p)}{\mathcal{X}^3}[\alpha'(r - r_1)(r - r_2)(r - r_3)],$$
$$= -\alpha r^3(r - r_a)(r - r_p)(r - r_1)(r - r_2)(r - r_3), \tag{59}$$

where $\alpha = -2M\alpha'/\mathcal{X}^3$. In principle, one can solve for r_1, r_2, and r_3 for different values of r_a and r_p. This way, we can obtain the resonant orbits for a spinning particle while neglecting the higher spin contribution, i.e., $\mathcal{O}(a^2)$, from the black hole. In the next discussion, we consider the Kerr black hole and numerically present the resonant orbits for a particle with spin.

3. Spinning particle: The Kerr spacetime

In this case, the radial potential within the linear spin approximation can be written as

$$V_s(r) = r^4[E^2 r^4 - (L_z^2 - a^2 E^2)r^2 + 2Mr(L_z - aE)^2 - (r^2 - 2Mr + a^2)r^2]$$
$$+ Sr^3\{2a^3 ME^2 - 4a^2 MEJ_z + 2aMJ_z^2 + 6aE^2 Mr^2 + 2EJ_z r^3 - 6EJ_z Mr^2\}$$
$$= r^3[r\{E^2 r^4 - (L_z^2 - a^2 E^2)r^2 + 2Mr(L_z - aE)^2 - (r^2 - 2Mr + a^2)r^2\}$$
$$+ S\{2a^3 ME^2 - 4a^2 MEJ_z + 2aMJ_z^2 + 6aE^2 Mr^2 + 2EJ_z r^3 - 6EJ_z Mr^2\}]$$
$$= -\alpha_s r^3(r - r_1)(r - r_2)(r - r_a)(r - r_p)(r - r_3), \tag{60}$$

and we now estimate each solution by equating the left- and right-hand sides. Therefore, we arrive at the following set of equations:

(1) From coefficient of r^5, we have $\alpha_s = 1 - E^2$.
(2) From coefficient of r^4, we manage to have

$$r_1 + r_2 + r_a + r_p + r_3 = \frac{2M}{\alpha_s}. \qquad (61)$$

(3) From coefficient of r^3, we have

$$a^2(E^2 - 1) - J_z^2 + 2EJ_zS$$
$$= -\alpha\{r_ar_p + r_1r_2 + (r_a + r_p)(r_1 + r_2)$$
$$+ r_3(r_1 + r_2 + r_a + r_p)\}. \qquad (62)$$

(4) From coefficient of r^2, we obtain

$$2Ma^2E^2 - 4aMEJ_z + 2MJ_z^2 + 6aE^2MS - 6EMSJ_z$$
$$= \alpha_s\{r_ar_pr_3 + (r_1 + r_2)(r_ar_p + r_3(r_a + r_p)).$$
$$+ r_1r_2(r_3 + r_a + r_p)\}. \qquad (63)$$

(5) From coefficient of r, we determine

$$r_2r_3r_ar_p + r_1r_3r_ar_p + r_1r_2\{r_ar_p + r_3(r_a + r_p)\}$$
$$= 0. \qquad (64)$$

(6) From the coefficient of r^0, we get

$$(2ME^2a^3 - 4MEJ_za^2 + 2MaJ_z^2)S = r_1r_2r_3r_ar_p\alpha_s. \qquad (65)$$

With $r_+ = r_1 + r_2$ and $r_\times = r_1r_2$, we can further compute E from Eq. (61),

$$E^2 = 1 - \frac{2M}{r_+ + r_a + r_p + r_3}. \qquad (66)$$

From Eq. (64), we can further compute r_3 as

$$r_3 = -\frac{r_\times r_ar_p}{r_\times(r_a + r_p) + r_ar_pr_+}. \qquad (67)$$

To obtain J_z, we can introduce the expression $X_\pm = 2Ma^2\times$ Eq. (62) $\pm$ Eq. (65) and with the $+$ sign, we arrive at

$$J_z^2 = a(a - S)(r_+ + r_a + r_p + r_3)^{-1}\{2a^2M[r_3(r_a + r_p)$$
$$+ r_ar_p + r_\times + r_+(r_a + r_p + r_3)] - 2Ma^4 - r_\times r_3r_ar_p$$
$$+ a^3S(r_a + r_p + r_3 + r_+ - 2M)\}. \qquad (68)$$

Along with the expressions X_- and Eq. (63), we can numerically solve for both r_1 and r_2 for given values of e and p. Therefore, whenever provided with r_a and r_p, we can compute energy and momentum corresponding to a spinning particle confined on the equatorial plane of the Kerr black hole. The next task is to determine the integral given in Eq. (11) and for a general Kerr spcatime, this is given in the Appendix. For convenience, we carry out the calculations within the linear framework of the spin parameter, while a general treatment shall be carried out elsewhere. In Figs. 5 and 6 we have shown resonant orbits for different orders of resonance while the angular momentum of the Kerr black hole varies accordingly. For a particle
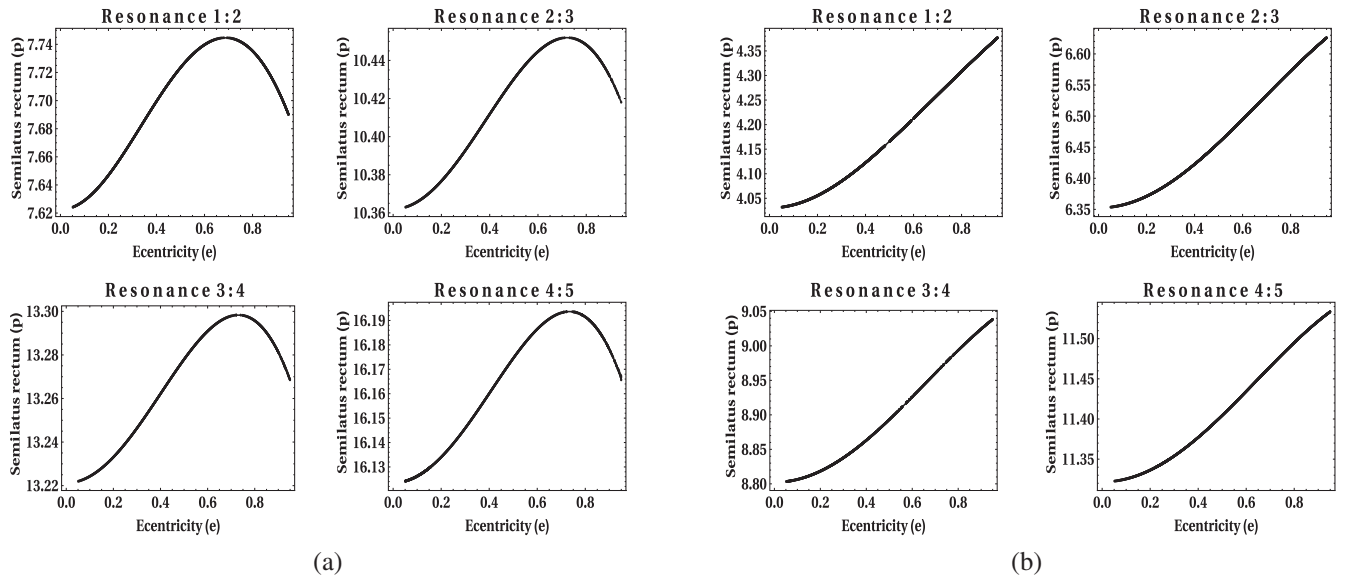

FIG. 5. $r\phi$ resonant orbits for particles with spin $S = 10^{-4}M$. The influence of different angular momentum of the black hole is also depicted. (a) Resonant orbits for a spinning particle in a black hole with angular momentum $a = 0:099M$. (b) Resonant orbits while the black hole has an angular momentum of $a = 0:9M$.
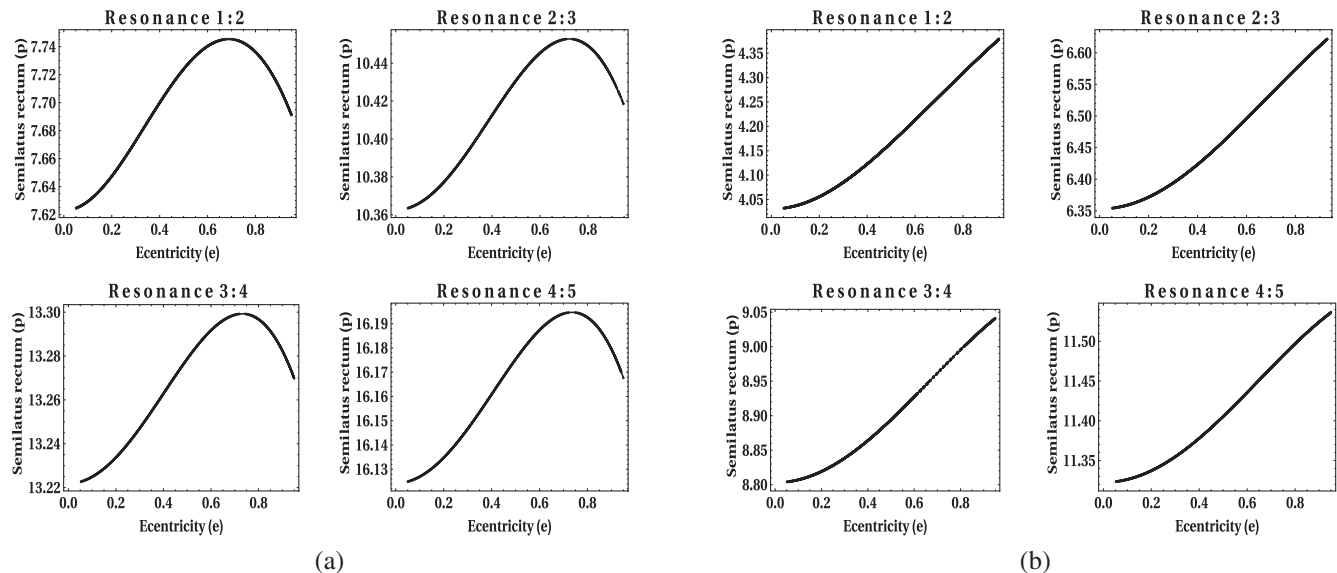
FIG. 6. $r\phi$ resonant orbits for particles with spin $S = -10^{-4}M$. The influence of different angular momentum of the black hole is also depicted. (a) Resonant orbits for a spinning particle in a black hole with angular momentum $a = 0\!:\!099M$. (b) Resonant orbits while the black hole has an angular momentum of $a = 0\!:\!9M$.

with spin $S = 10^{-4}M$, various resonant orbits for $a = 0.099M$ and $a = 0.9M$ are given in Figs. 5(a) and 5(b) respectively. The studies related to spin $S = -10^{-4}M$ are shown in Fig. 6 for different resonance and the black hole's momentum.

VI. CONCLUDING REMARKS

In the present article we have studied the trajectories of a spinning particle and discussed their orbital resonance in the Kerr background. We typically explore two particular events: first, the resonance in between small oscillation frequencies, and second, $r\phi$ resonance on the equatorial plane of the Kerr black hole. In the case of a spinning particle, the off-equatorial trajectories are not easily derivable and can hardly be written in a convenient analytical form. Therefore, in the present context, we have only considered the $r\phi$ resonance and were mostly concerned with locating the resonant orbits for different spin parameters. We confined our discussions for a pole-dipole particle, i.e., a particle with nonzero dipole moment while all the higher order moments are set to zero. In addition, the entire study is only valid for a linearized spin parameter and any contributions that appear at $\mathcal{O}(S^2)$ and higher are ignored for convenience. The key findings of the present article can be summarized as follows.

The first part of the paper deals with the nearly circular orbits hobbling around the equatorial plane, for an extended object around the Kerr black hole. In the presence of nonvanishing spin, the expressions for small oscillation frequencies would change and therefore, the locations of resonant orbits would also shift. For our study, we

employed the analytical expressions for frequencies given by Hinderer *et al.* in Ref. [63] and obtained the locations of the resonant orbits for different angular momentum of the black hole. In the case of corotating orbits, we discussed all three resonance phenomena, i.e., $r\theta$, $r\phi$, and $\theta\phi$, given in Figs. 1(a)–1(c) respectively, for various spin parameters of the secondary object. On the other hand, the resonant orbits for the counterrotating case is demonstrated in Fig. 2. The $r\theta$, $r\phi$, and $\phi\theta$ resonances are shown in Figs. 2(a)–2(c), respectively. In order to preserve the convention given in Eq. (11), we address the resonance between θ and ϕ to be $\phi\theta$, rather than $\theta\phi$. As expected, within the linear spin approximation, the difference in location between geodesic and spinning particle is infinitesimal.

The second part deals with the $r\phi$ resonance considering the trajectories are completely confined on the equatorial plane. We locate the resonant orbits for different values of the black hole's momentum as well as the particle's spin. When the angular momentum of the black hole is small, the resonant orbits have a weak dependency on the eccentricity e. It is explicitly demonstrated in Figs. 5(a) and 6(a). However, the e dependency increases as one increases the value of angular momentum of the black hole as it is shown in Figs. 5(b) and 6(b). The nature of resonant orbits are also largely effected by the black hole rotation as depicted in Figs. 5 and 6. For a small or no rotation of the black hole [Figs. 3, 5(a), and 6(a)], the semilatus rectum steadily increases with the eccentricity e and attains a maximum value for a particular eccentricity say $e = e_{\max}$. Further increase in the eccentricity would result in the decrease of the semilatus rectum p as shown in Figs. 3, 5(a), and 6(a). On the other hand, for black holes with larger angular

momentum, p steadily increases with the eccentricity e and attains the highest value as e approaches unity. Furthermore, the orbits shift towards the event horizon as one either increases the momentum of the black hole or decreases the order of resonance.

Finally, it should be emphasized that the change in locations for different spin parameters within the linear approximation is infinitesimally small and nearly indistinguishable. Therefore, it would be important to investigate for large spin parameters of the secondary object. However, the immediate followup of the present work would be to consider the $r\theta$ resonance which requires a numerical framework.

ACKNOWLEDGMENTS

APPENDIX: DETAIL CALCULATIONS TO OBTAIN THE RESONANT ORBITS

In the Kerr black hole, we obtain

$$\frac{\mathcal{U}^3}{\mathcal{U}^1} = \frac{d\phi}{dr} = \frac{r^2\{J_z - (a+S)E\} + \frac{aP_s r^2}{\Delta}}{[V_s(r)]^{1/2}}, \quad (A1)$$

with $V_s(r) = -\alpha_s r^3(r-r_1)(r-r_2)(r-r_a)(r-r_p)(r-r_3)$. We can split the above integration into two parts, the first one is $\mathcal{G}$ and second one is $\mathcal{R}$ and these are given as

$$\mathcal{G} = \frac{r^2\{J_z - (a+S)E\}}{[V_s(r)]^{1/2}} = \frac{r\{J_z - (a+S)E\}}{[-\alpha_s(r-0)(r-r_1)(r-r_2)(r-r_a)(r-r_p)(r-r_3)]^{1/2}},$$

$$\mathcal{R} = \frac{ar^2P_s}{\Delta[V_s(r)]^{1/2}} = \frac{a\{Er^3 + ar(a+S-J_z) + MS(a-J_z)\}}{(r-r_H^+)(r-r_H^-)[-\alpha_s(r-0)(r-r_1)(r-r_2)(r-r_a)(r-r_p)(r-r_3)]^{1/2}}, \quad (A2)$$

where r_H^+ and r_H^- are given as the outer and inner horizon respectively. Furthermore, with the substitution [65]

$$r = \frac{(r_a + r_p) + x(r_a - r_p)}{2}, \quad (A3)$$

we arrive at the following expression:

$$\frac{d\phi}{dx} = \frac{r_a - r_p}{2}\frac{d\phi}{dr} = \frac{r_a - r_p}{2}(\mathcal{G}_x + \mathcal{R}_x). \quad (A4)$$

The $\mathcal{G}$ becomes $\mathcal{G}_x$ and given as

$$\mathcal{G}_x = \frac{r_x\{J_z - (a+S)E\}}{[-\alpha_s(r_x - 0)(r_x - r_1)(r_x - r_2)(r_x - r_a)(r_x - r_p)(r_x - r_3)]^{1/2}}. \quad (A5)$$

By using the fact,

$$r_x - r_i = \frac{r_a + r_p - 2r_i}{2}(1 + K_i x), \quad (A6)$$

with $K_i = \frac{r_a - r_p}{r_a + r_p - 2r_i}$ where i runs from 0 to 3 and $r_0 = 0$, the above equation reads as

$$\mathcal{G}_x = \frac{1}{2}(r_a + r_p)(1 + K_0 x)\{J_z - (a+S)E\}\{2^{-6}\alpha_s(1 - x^2)(1 + K_0 x)(1 + K_1 x)(1 + K_2 x)(1 + K_3 x)$$
$$\times (r_a + r_p)(r_a - r_p)^2(r_a + r_p - 2r_1)(r_a + r_p - 2r_2)(r_a + r_p - 2r_3)\}^{-1/2},$$
$$= \frac{N_k(1 + K_0 x)\{J_z - (a+S)E\}}{\sqrt{[(1 - x^2)(1 + K_0 x)(1 + K_1 x)(1 + K_2 x)(1 + K_3 x)]}}. \quad (A7)$$

In the above, we assume

$$N_{\mathrm{k}} = \frac{4(r_a + r_p)}{\sqrt{[\alpha(r_a + r_p)(r_a - r_p)^2(r_a + r_p - 2r_1)(r_a + r_p - 2r_2)(r_a + r_p - 2r_3)]}} = \frac{2\langle N_{\mathrm{k}}\rangle}{r_a - r_p}, \tag{A8}$$

with

$$\langle N_{\mathrm{k}}\rangle = \frac{2(r_a + r_p)}{\sqrt{[\alpha_{\mathrm{s}}(r_a + r_p)(r_a + r_p - 2r_1)(r_a + r_p - 2r_2)(r_a + r_p - 2r_3)]}}. \tag{A9}$$

Therefore, we can finally write

$$\mathcal{G}_x = \frac{2\langle N_{\mathrm{k}}\rangle}{r_a - r_p} \frac{(1 + K_0 x)\{J_z - (a + S)E\}}{\sqrt{[(1 - x^2)(1 + K_0 x)(1 + K_1 x)(1 + K_2 x)(1 + K_3 x)]}}. \tag{A10}$$

The other part can be written as

$$\begin{aligned}
\mathcal{R}_x &= \frac{a\{Er_x^3 + ar_x(a + S - J_z) + MS(a - J_z)\}}{(r_x - r_{\mathrm{H}}^+)(r_x - r_{\mathrm{H}}^-)[-\alpha_{\mathrm{s}}(r_x - 0)(r_x - r_1)(r_x - r_2)(r_x - r_a)(r_x - r_p)(r_x - r_3)]^{1/2}}, \\
&= \frac{a}{\Delta} Er_x^3 + a(a + S - J_z)r_x + MS(a - J_z)\{2^{-6}\alpha_{\mathrm{s}}(1 - x^2)(1 + K_0 x)(1 + K_1 x)(1 + K_2 x)(1 + K_3 x) \\
&\quad \times (r_a + r_p)(r_a - r_p)^2(r_a + r_p - 2r_1)(r_a + r_p - 2r_2)(r_a + r_p - 2r_3)\}^{-1/2}, \\
&= \frac{2}{r_a - r_p} \frac{4a \times 4}{(r_a + r_p - 2r_{\mathrm{H}}^+)(r_a + r_p - 2r_{\mathrm{H}}^-)(1 + K_{\mathrm{H}}^+ x)(1 + K_{\mathrm{H}}^- x)} \\
&\quad \times \frac{1}{\sqrt{\alpha_{\mathrm{s}}(r_a + r_p)(r_a + r_p - 2r_1)(r_a + r_p - 2r_2)(r_a + r_p - 2r_3)}} \\
&\quad \times \frac{Er_x^3 + a(a + S - J_z)r_x + MS(a - J_z)}{(1 + K_{\mathrm{H}}^+ x)(1 + K_{\mathrm{H}}^- x)\sqrt{(1 - x^2)(1 + K_0 x)(1 + K_1 x)(1 + K_2 x)(1 + K_3 x)}}, \\
&= \frac{2\langle \bar{N}_{\mathrm{k}}\rangle}{r_a - r_p} \frac{E(1 - K_0 x)^3(r_a + r_p)^3 + 4a(a + S - J_z)(r_a + r_p)(1 - K_0 x) + 8MS(a - J_z)}{8(1 + K_{\mathrm{H}}^+ x)(1 + K_{\mathrm{H}}^- x)\sqrt{(1 - x^2)(1 + K_0 x)(1 + K_1 x)(1 + K_2 x)(1 + K_3 x)}},
\end{aligned} \tag{A11}$$

where we assume

$$\begin{aligned}
\langle \bar{N}_{\mathrm{k}}\rangle &= \frac{4a \times 4}{(r_a + r_p - 2r_{\mathrm{H}}^+)(r_a + r_p - 2r_{\mathrm{H}}^-)(1 + K_{\mathrm{H}}^+ x)(1 + K_{\mathrm{H}}^- x)} \\
&\quad \times \frac{Er_x^3 + a(a + S - J_z)r_x + MS(a - J_z)}{(1 + K_{\mathrm{H}}^+ x)(1 + K_{\mathrm{H}}^- x)\sqrt{(1 - x^2)(1 + K_0 x)(1 + K_1 x)(1 + K_2 x)(1 + K_3 x)}}.
\end{aligned} \tag{A12}$$

The final equation can now be written as

$$\begin{aligned}
\frac{d\phi}{dx} &= \langle N_{\mathrm{k}}\rangle \frac{(1 + K_0 x)\{J_z - (a + S)E\}}{\sqrt{[(1 - x^2)(1 + K_0 x)(1 + K_1 x)(1 + K_2 x)(1 + K_3 x)]}} \\
&\quad + \langle \bar{N}_{\mathrm{k}}\rangle \frac{E(1 - K_0 x)^3(r_a + r_p)^3 + 4a(a + S - J_z)(r_a + r_p)(1 - K_0 x) + 8MS(a - J_z)}{8(1 + K_{\mathrm{H}}^+ x)(1 + K_{\mathrm{H}}^- x)\sqrt{(1 - x^2)(1 + K_0 x)(1 + K_1 x)(1 + K_2 x)(1 + K_3 x)}}.
\end{aligned} \tag{A13}$$

By employing the fact, $\sqrt{(1 + K_0 x)(1 + K_1 x)} = 1 + \frac{(K_0 + K_1)}{2} x = 1 + \bar{K}_1 x$ and $\sqrt{(1 + K_2 x)(1 + K_3 x)} = 1 + \bar{K}_2 x$, the above equation can be written as

$$\frac{d\phi}{dx} = \langle N_k \rangle \frac{(1 + K_0 x)\{J_z - (a + S)E\}}{\sqrt{1 - x^2}(1 + \bar{K}_1 x)(1 + \bar{K}_2 x)}$$
$$+ \langle \overline{N_k} \rangle \frac{E(1 - K_0 x)^3 (r_a + r_p)^3 + 4a(a + S - J_z)(r_a + r_p)(1 - K_0 x) + 8MS(a - J_z)}{8\sqrt{(1 - x^2)}(1 + K_H^+ x)(1 + K_H^- x)(1 + \bar{K}_1 x)(1 + \bar{K}_2 x)}. \tag{A14}$$

We further write

$$\frac{1}{(1 + \bar{K}_1 x)(1 + \bar{K}_2 x)} = \frac{1}{\bar{K}_2 - \bar{K}_1} \left\{ \frac{\bar{K}_2}{1 + \bar{K}_2 x} - \frac{\bar{K}_1}{1 + \bar{K}_1 x} \right\}, \tag{A15}$$

and also

$$\frac{1}{(1 + K_H^+ x)(1 + K_H^- x)(1 + \bar{K}_1 x)(1 + \bar{K}_2 x)} = \frac{A}{1 + K_H^+ x} + \frac{B}{1 + K_H^- x} + \frac{C}{1 + \bar{K}_1 x} + \frac{D}{1 + \bar{K}_2 x}, \tag{A16}$$

with A, B, C and D has the following expressions:

$$A = \frac{(K_H^+)^3}{(K_H^+ - K_H^-)(K_H^+ - \bar{K}_1)(K_H^+ - \bar{K}_2)}, \qquad B = \frac{(K_H^-)^3}{(K_H^- - K_H^+)(K_H^- - \bar{K}_1)(K_H^- - \bar{K}_2)},$$
$$C = \frac{(\bar{K}_1)^3}{(\bar{K}_1 - K_H^+)(\bar{K}_1 - K_H^-)(\bar{K}_1 - \bar{K}_2)}, \qquad D = \frac{(\bar{K}_2)^3}{(\bar{K}_2 - K_H^+)(\bar{K}_2 - K_H^-)(\bar{K}_2 - \bar{K}_1)}. \tag{A17}$$

With all the above machinery employed, we arrive at the following expression:

$$\frac{d\phi}{dx} = \langle N_k \rangle \frac{\{J_z - (a + S)E\}}{\bar{K}_2 - \bar{K}_1} \left\{ \frac{\bar{K}_2(1 + K_0 x)}{\sqrt{1 - x^2}(1 + \bar{K}_2 x)} - \frac{\bar{K}_1(1 + K_0 x)}{\sqrt{1 - x^2}(1 + \bar{K}_1 x)} \right\}$$
$$+ \frac{\langle \overline{N_k} \rangle}{8} \left\{ E(r_a + r_p)^3 \left(\frac{A(1 - K_0 x)^3}{\sqrt{(1 - x^2)}(1 + K_H^+ x)} + \frac{B(1 - K_0 x)^3}{\sqrt{(1 - x^2)}(1 + K_H^- x)} \right. \right.$$
$$\left. \left. + \frac{C(1 - K_0 x)^3}{\sqrt{(1 - x^2)}(1 + \bar{K}_1 x)} + \frac{D(1 - K_0 x)^3}{\sqrt{(1 - x^2)}(1 + \bar{K}_2 x)} \right) \right\} + \frac{\langle \overline{N_k} \rangle a(a + S - J_z)(r_a + r_p)}{2}$$
$$\times \left\{ \frac{A(1 - K_0 x)}{\sqrt{(1 - x^2)}(1 + K_H^+ x)} + \frac{B(1 - K_0 x)}{\sqrt{(1 - x^2)}(1 + K_H^- x)} + \frac{C(1 - K_0 x)}{\sqrt{(1 - x^2)}(1 + \bar{K}_1 x)} + \frac{D(1 - K_0 x)}{\sqrt{(1 - x^2)}(1 + \bar{K}_2 x)} \right\}$$
$$+ MS(a - J_z)\langle \overline{N_k} \rangle \left\{ \frac{A}{\sqrt{(1 - x^2)}(1 + K_H^+ x)} + \frac{B}{\sqrt{(1 - x^2)}(1 + K_H^- x)} \right.$$
$$\left. + \frac{C}{\sqrt{(1 - x^2)}(1 + \bar{K}_1 x)} + \frac{D}{\sqrt{(1 - x^2)}(1 + \bar{K}_2 x)} \right\}. \tag{A18}$$

Now we have to do the calculation $\int_{-1}^{1} \left(\frac{d\phi}{dx} \right) dx$ and to do so, we have used the following equations:

$$I_1(K) = \int_{-1}^{1} \frac{dx}{\sqrt{1 - x^2}(1 + Kx)} = \frac{\pi}{\sqrt{1 - K^2}},$$
$$I_2(K) = \int_{-1}^{1} \frac{(1 + K_0 x)dx}{\sqrt{1 - x^2}(1 + Kx)} = \frac{\pi}{K} \left\{ \frac{K - K_0}{\sqrt{1 - K^2}} + K_0 \right\},$$
$$I_3(K) = \int_{-1}^{1} \frac{(1 + K_0 x)^3 dx}{\sqrt{1 - x^2}(1 + Kx)} = \frac{\pi}{K^3} \left\{ \frac{(K - K_0)^3}{\sqrt{1 - K^2}} - \left[(K - K_0)^3 - \frac{K^2(K_0^3 + 2K)}{2} \right] \right\}. \tag{A19}$$

With the above information, we can write the final equation as follows:

$$
\begin{aligned}
\int_{-1}^{1} \frac{d\phi}{dx} dx = {} & \langle N_{\mathrm{k}} \rangle \frac{\{J_z - (a+S)E\}}{\bar{K}_2 - \bar{K}_1} \{\bar{K}_2 I_2(\bar{K}_2) - \bar{K}_1 I_2(\bar{K}_1)\} \\
& + \frac{\langle \overline{N_{\mathrm{k}}} \rangle}{8} \{E(r_a + r_p)^3 [AI_3(K_{\mathrm{H}}^+) + BI_3(K_{\mathrm{H}}^-) + CI_3(\bar{K}_1) + DI_3(\bar{K}_2)]\} \\
& + \frac{\langle \overline{N_{\mathrm{k}}} \rangle a(a+S-J_z)(r_a + r_p)}{2} \{AI_2(K_{\mathrm{H}}^+) + BI_2(K_{\mathrm{H}}^-) + CI_2(\bar{K}_1) + DI_2(\bar{K}_2)\} \\
& + MS(a - J_z)\langle \overline{N_{\mathrm{k}}} \rangle \{AI_1(K_{\mathrm{H}}^+) + BI_1(K_{\mathrm{H}}^-) + CI_1(\bar{K}_1) + DI_1(\bar{K}_2)\}.
\end{aligned}
\tag{A20}
$$

[1] A. Einstein, Erklarung der perihelionbewegung der merkur aus der allgemeinen relativitatstheorie, Sitzungsber. Preuss. Akad. Wiss. Phys. Math. Kl. **47,** 831 (1915).

[2] A. Einstein, *The Meaning of Relativity,* 5th ed. (Princeton University Press, Princeton, NJ, 2004).

[3] C. M. Will, *Theory and Experiment in Gravitational Physics* (Cambridge University Press, Cambridge, England, 1993).

[4] J. Brink, M. Geyer, and T. Hinderer, Orbital Resonances around Black Holes, Phys. Rev. Lett. **114,** 081102 (2015).

[5] J. Brink, M. Geyer, and T. Hinderer, Astrophysics of resonant orbits in the Kerr metric, Phys. Rev. D **91,** 083001 (2015).

[6] S. Suzuki and K.-I. Maeda, Chaos in Schwarzschild space-time: The motion of a spinning particle, Phys. Rev. D **55,** 4848 (1997).

[7] J. M. Bardeen, W. H. Press, and S. A. Teukolsky, Rotating black holes: Locally nonrotating frames, energy extraction, and scalar synchrotron radiation, Astrophys. J. **178,** 347 (1972).

[8] B. O'Neil, *The Geometry of Kerr Black Holes* (A K Peters, Wellesley, MA, 1995).

[9] J. Levin and G. Perez-Giz, A periodic table for black hole orbits, Phys. Rev. D **77,** 103005 (2008).

[10] R. Grossman, J. Levin, and G. Perez-Giz, The harmonic structure of generic Kerr orbits, Phys. Rev. D **85,** 023012 (2012).

[11] K. Danzmann, T. A. Prince, P. Binetruy, P. Bender, S. Buchman, J. Centrella, M. Cerdonio, N. Cornish, M. Cruise, C. J. Cutler *et al.,* LISA: Unveiling a hidden universe, Assessment Study Report ESA/SRE, 2011.

[12] C. F. Sopuerta, Probing the strong gravity regime with eLISA: Progress on EMRIs, ASP Conf. Ser. **467,** 69 (2013).

[13] M. Armano *et al.,* Sub-Femto- g Free Fall for Space-Based Gravitational Wave Observatories: LISA Pathfinder Results, Phys. Rev. Lett. **116,** 231101 (2016).

[14] M. Mathisson, Neue mechanik materieller systemes, Acta Phys. Pol. **6,** 163 (1937).

[15] A. Papapetrou, Spinning test particles in general relativity. 1., Proc. R. Soc. A **209,** 248 (1951).

[16] W. G. Dixon, Dynamics of extended bodies in general relativity. I. Momentum and angular momentum, Proc. R. Soc. A **314,** 499 (1970).

[17] W. G. Dixon, Dynamics of extended bodies in general relativity—II. Moments of the charge-current vector, Proc. R. Soc. A **319,** 509 (1970).

[18] W. G. Dixon, Dynamics of extended bodies in general relativity—III. Equations of motion, Phil. Trans. R. Soc. A **277,** 59 (1974).

[19] A. Papapetrou and W. Ubich, Das pol-dipol-teilchen im gravitationsfeld und elektromagnetischen feld, Z. für Naturforsch. A **10,** 109 (1955).

[20] R. Hojman and S. Hojman, Spinning charged test particles in a Kerr-Newman background, Phys. Rev. D **15,** 2724 (1977).

[21] P. I. Jefremov, O. Yu. Tsupko, and G. S. Bisnovatyi-Kogan, Innermost stable circular orbits of spinning test particles in Schwarzschild and Kerr space-times, Phys. Rev. D **91,** 124030 (2015).

[22] R. Plyatsko and M. Fenyk, Highly relativistic circular orbits of spinning particle in the Kerr field, Phys. Rev. D **87,** 044019 (2013).

[23] J. Ehlers and E. Rudolph, Dynamics of extended bodies in general relativity center-of-mass description and quasirigidity, Gen. Relativ. Gravit. **8,** 197 (1977).

[24] W. Dixon, A covariant multipole formalism for extended test bodies in general relativity, Nuovo Cimento (1955–1965) **34,** 317 (1964).

[25] O. Semerak, Spinning particles in vacuum spacetimes of different curvature types, Phys. Rev. D **92,** 064032 (2015).

[26] K. Kyrian and O. Semerak, Spinning test particles in a Kerr field, Mon. Not. R. Astron. Soc. **382,** 1922 (2007).

[27] F. Costa, C. A. R. Herdeiro, J. Natario, and M. Zilhao, Mathisson's helical motions for a spinning particle: Are they unphysical?, Phys. Rev. D **85,** 024001 (2012).

[28] L. F. O. Costa, G. Lukes-Gerakopoulos, and O. Semerák, On spinning particles in general relativity: Momentum-velocity relation for the Mathisson-Pirani spin condition, Phys. Rev. D **97,** 084023 (2018).

[29] G. Lukes-Gerakopoulos, J. Seyrich, and D. Kunst, Investigating spinning test particles: Spin supplementary conditions and the Hamiltonian formalism, Phys. Rev. D **90,** 104019 (2014).

[30] T. Tanaka, Y. Mino, M. Sasaki, and M. Shibata, Gravitational waves from a spinning particle in circular orbits around a rotating black hole, Phys. Rev. D **54,** 3762 (1996).

[31] E. Corinaldesi and A. Papapetrou, Spinning test particles in general relativity. II, in *Nonlinear Gravitodynamics: The Lense-Thirring Effect* (World Scientific, Singapore, 2003), pp. 404–413.

[32] M. Saijo, K.-I. Maeda, M. Shibata, and Y. Mino, Gravitational waves from a spinning particle plunging into a Kerr black hole, Phys. Rev. D **58,** 064005 (1998).

[33] S. Mukherjee, Periastron shift for a spinning test particle around naked singularities, Phys. Rev. D **97,** 124006 (2018).

[34] S. Mukherjee and K. Rajesh Nayak, Off-equatorial stable circular orbits for spinning particles, Phys. Rev. D **98,** 084023 (2018).

[35] S. Mukherjee, Collisional Penrose process with spinning particles, Phys. Lett. B **778,** 54 (2018).

[36] A. A. Deriglazov and W. Guzmán Ramírez, Recent progress on the description of relativistic spin: Vector model of spinning particle and rotating body with gravimagnetic moment in general relativity, Adv. Theor. Math. Phys. **2017,** 7397159 (2017).

[37] A. A. Deriglazov and W. Guzmán Ramírez, Frame-dragging effect in the field of nonrotating body due to unit gravimagnetic moment, Phys. Lett. B **779,** 210 (2018).

[38] O. Semerak, Spinning test particles in a Kerr field. 1., Mon. Not. R. Astron. Soc. **308,** 863 (1999).

[39] J. Steinhoff, Spin gauge symmetry in the action principle for classical relativistic particles, arXiv:1501.04951.

[40] O. Semerak, Spinning particles in vacuum spacetimes of different curvature types: Natural reference tetrads, and massless particles, Phys. Rev. D **92,** 124036 (2015).

[41] S. Babak, J. R. Gair, and R. H. Cole, Extreme mass ratio inspirals: Perspectives for their detection, Fund. Theor. Phys. **179,** 783 (2015).

[42] N. Bajaj, *The Physics of Waves and Oscillations* (Tata McGraw-Hill Education, New York, 1988).

[43] B. Carter, Killing horizons and orthogonally transitive groups in space-time, J. Math. Phys. (N.Y.) **10,** 70 (1969).

[44] K. Rosquist, T. Bylund, and L. Samuelsson, Carter's constant revealed, Int. J. Mod. Phys. D **18,** 429 (2009).

[45] S. Mukherjee and K. Rajesh Nayak, Carter constant and angular momentum, Int. J. Mod. Phys. D **27,** 1750180 (2018).

[46] V. Witzany, Spin-perturbed orbits near black holes, arXiv:1903.03649.

[47] V. Witzany, Hamilton-Jacobi equation for spinning particles near black holes, Phys. Rev. D **100,** 104030 (2019).

[48] G. W. Gibbons, R. H. Rietdijk, and J. W. van Holten, SUSY in the sky, Nucl. Phys. **B404,** 42 (1993).

[49] D. Kunst, T. Ledvinka, G. Lukes-Gerakopoulos, and J. Seyrich, Comparing Hamiltonians of a spinning test particle for different tetrad fields, Phys. Rev. D **93,** 044004 (2016).

[50] G. Lukes-Gerakopoulos, M. Katsanikas, P. A. Patsis, and J. Seyrich, The dynamics of a spinning particle in a linear in spin Hamiltonian approximation, Phys. Rev. D **94,** 024024 (2016).

[51] O. Zelenka, G. Lukes-Gerakopoulos, V. Witzany, and O. Kopacek, Growth of resonances and chaos for a spinning test particle in the Schwarzschild background, Phys. Rev. D **101,** 024037 (2020).

[52] V. Arnold, Proof of a theorem of A. N. Kolmogorov on the invariance of quasi-periodic motions under small perturbations of the Hamiltonian (Kolmogoroff theorem on invariance of quasi-periodic motions under small perturbations of Hamiltonian), Russ. Math. Surv. **18,** 9 (1963).

[53] V. Arnold, Small denominators. II. Proof of a theorem of an kolmogorov on the invariance of quasi-periodic motions under small perturbations of the Hamiltonian, Russ. Math. Surv. **18,** 9 (1963).

[54] J. Moser, Stable and random motions in dynamical systems, *Ann. Math. Studies 77* (Princeton University Press, Princeton, 1973).

[55] C. P. L. Berry, R. H. Cole, P. Cañizares, and J. R. Gair, Importance of transient resonances in extreme-mass-ratio inspirals, Phys. Rev. D **94,** 124042 (2016).

[56] M. van de Meent, Resonantly enhanced kicks from equatorial small mass-ratio inspirals, Phys. Rev. D **90,** 044027 (2014).

[57] C. M. Hirata, Resonant recoil in extreme mass ratio binary black hole mergers, Phys. Rev. D **83,** 104024 (2011).

[58] U. Ruangsri, S. J. Vigeland, and S. A. Hughes, Gyroscopes orbiting black holes: A frequency-domain approach to precession and spin-curvature coupling for spinning bodies on generic Kerr orbits, Phys. Rev. D **94,** 044008 (2016).

[59] W. Tulczyjew, Motion of multipole particles in general relativity theory, Acta Phys. Pol. **18,** 393 (1959).

[60] G. Lukes-Gerakopoulos, Time parametrizations and spin supplementary conditions of the Mathisson-Papapetrou-Dixon equations, Phys. Rev. D **96,** 104023 (2017).

[61] R. Rudiger, Conserved quantities of spinning test particles in general relativity. I., Proc. R. Soc. A **375,** 185 (1981).

[62] R. Rudiger, Conserved quantities of spinning test particles in general relativity. II., Proc. R. Soc. A **385,** 229 (1983).

[63] T. Hinderer *et al.*, Periastron advance in spinning black hole binaries: Comparing effective-one-body and numerical relativity, Phys. Rev. D **88,** 084005 (2013).

[64] C. Cutler, D. Kennefick, and E. Poisson, Gravitational radiation reaction for bound motion around a Schwarzschild black hole, Phys. Rev. D **50,** 3816 (1994).

[65] D. Kunst, V. Perlick, and C. Lammerzahl, Isofrequency pairing of spinning particles in Schwarzschild-de Sitter spacetime, Phys. Rev. D **92,** 024029 (2015).

[66] A. Y. Sochnev, Approximation of ultra-elliptic and elliptic integrals without infinite series expansion of the integrands, Ukrainian Mathematical Journal **20,** 442 (1968).

[67] R. M. Wald, *General Relativity* (University of Chicago Press, Chicago, 1984), p. 504.